

Optical approach for monitoring the periodontal ligament changes induced by orthodontic forces around maxillary anterior teeth of white rats

Jihoon Na · Byeong Ha Lee · Jae Ho Baek · Eun Seo Choi

Received: 29 December 2006 / Accepted: 7 December 2007 / Published online: 5 February 2008
© International Federation for Medical and Biological Engineering 2008

Abstract Structural variations of the periodontal ligament (PDL) induced by orthodontic forces have been evaluated by optical coherence tomography (OCT) and compared to images obtained by conventional radiography. Here, two specially designed orthodontic appliances were installed on the maxillary anterior teeth of white rats for applying different magnitudes of orthodontic forces. Constant distraction force magnitudes of 0, 5, 10, and 30 gf were given to four respective rats over a period of 5 days. At the end of the treatment period, the rats were sacrificed and the maxillaries were extracted for X-ray and OCT imaging. The PDL variations, proportional to the force magnitude, were clearly indicated in the OCT measurements. The OCT images further showed that the ligament was torn for a constant orthodontic force of 30 gf. These results support the clinical dental application of OCT for

monitoring the ligament changes during orthodontic procedures. The real-time imaging capability of OCT, together with its high resolution, has the potential to help dentists with in vivo orthodontic treatments in human subjects as well.

Keywords Optical coherence tomography · Periodontal ligament · Periodontium · Dentistry · Medical optics instrument · Clinical application

Abbreviations

OCT Optical coherence tomography
PDL Periodontal ligament
SD Sprague–Dawley

1 Introduction

Orthodontic tooth movement is associated with biological reactions within the periodontal ligament (PDL) and the alveolar bone [13, 17, 19]. For this reason, there is a strong requirement for the development of precise diagnostic tools to detect and characterize tooth movement during orthodontic procedures by monitoring PDL responses to treatment. During the treatment process, it is important to select the most appropriate mechanical properties of orthodontic devices to avoid any side effects, discomfort, or PDL damage [23]. Improper appliances can cause patients to suffer from periodontal diseases, and inadequate biomechanical consideration has the potential to cause various side effects during teeth adjustments, which are controlled by a series of bone resorption and apposition. To this end, several researchers [2, 18, 19] have studied the optimal conditions for tooth movement

J. Na · B. H. Lee (✉)
Department of Information and Communications,
Gwangju Institute of Science and Technology (GIST),
1 Oryong-dong, Buk-gu, Gwangju 500-712, South Korea
e-mail: leebh@gist.ac.kr

J. Na
e-mail: jhna@gist.ac.kr

J. H. Baek
Department of Orthodontics, Division of Dentistry,
Ulsan University Hospital, 290-3 Jeonha-dong,
Dong-gu, Ulsan, South Korea
e-mail: baek@baekorthodontics.com

E. S. Choi
Department of Physics, Chosun University,
375 Seosuk-dong, Dong-gu,
Gwangju 501-759, South Korea
e-mail: cesman@chosun.ac.kr

with various animal tests, and concluded that it was very difficult to perform an accurate analysis of the correlation between tooth movement and the magnitude of the applied orthodontic force.

Conventional radiography [26] is one of the most popular diagnostic imaging tools in clinical dentistry. The utility of radiography, however, is limited due to its relatively low axial resolution, and by the fact that radiography provides only an overlapped two-dimensional image, making an interactive rapid therapeutic response during orthodontic treatment considerably difficult. Although 3D computed tomography (CT) has been introduced to overcome these weaknesses, there is one further intrinsic limitation in radiography, the danger of irradiation. Thus, the development of an imaging modality that can support functions such as high axial-resolution and real-time monitoring during treatment is a potential solution for preventing these negative effects, increasing the efficiency of treatment, and reducing the treatment time.

In terms of anatomy, PDL is a thin and fibrous ligament mainly composed of collagen, which connects the tooth to its bony socket [3]. Since it is the first area from which sequential reactions start when an external force is applied, the critical tolerable level of the force that can be applied during orthodontic treatment should be identified by monitoring its response to a range of applied forces. However, there has been no appropriate tool made clinically available to measure the orthodontic forces required for maintaining the homeostasis of the teeth and their surrounding tissues; unfortunately, there is no confirmable clinical criteria for safety established yet, either.

Optical coherence tomography (OCT) is a medical diagnostic imaging modality that can provide a noninvasive two-dimensional [11] or three-dimensional [15, 25] image of biomedical tissues with a high resolution. OCT has been studied in terms of its use in such medical research fields as ophthalmology [20], dentistry [4, 8, 14, 24], gastroenterology [10], urology [21], and gynecology [9], and endoscopic probes for OCT have been attempted in various fields of applications [9, 22]. In addition, to enhance the performance of optical biopsies based on OCT images, a Fourier or spectral domain OCT has also been studied [5, 7].

In this article, we present the results of our study on PDL variation under orthodontic forces by using both conventional X-ray and OCT imaging. Here, specially designed appliances were employed to apply different magnitudes of force on the maxillary anterior teeth of white rats [10 weeks old, Sprague–Dawley (SD) rats, male]. Then, the OCT and X-ray radiographic images used for comparison were obtained under distraction tooth movement.

2 Materials and methods

2.1 Orthodontic appliances

The orthodontic appliances were designed and constructed using small pieces of orthodontic memory-form-wire and resin. By using metal wires having different diameters, the adjustment of the orthodontic force to the teeth could be easily done when similar bending was applied. The springs seen in Fig. 1 were partially covered with a light curable hard resin (BISFILTM CORE, Bisco, Inc., USA) to maintain the bend of the spring, which was designed to apply a constant magnitude of force on a sample during the experiment. Table 1 classifies the groups depending on the force magnitudes and type of appliance; the constant orthodontic force magnitudes were classified as four force-based groups [control (0 gf), light (5 gf), medium (10 gf), and heavy (30 gf)] to evaluate the PDL structure under distraction tooth movement.

Specially designed brackets having a center hole 0.7 mm in diameter were used in this study, with a light curable bonding resin (Light Bond[®], Reliance Ortho Prod. Inc., USA) being used to fix the appliances, as shown in Fig. 1d. The springs transferring the orthodontic forces to the brackets were made with Ni–Ti wires that had different diameters to enable the control of different force magnitudes. These springs were installed into the holes of the brackets on the maxillary anterior tooth and fixed with a light curable resin (FiltekTM Flow, 3M ESPE), as shown in Fig. 2. Figure 1 presents photographs showing the designed appliances used in this experiment; the arrows shown in Fig. 1a–c indicate the orthodontic force directions applied to the samples.

2.2 Preparation of the rats

We selected four white rats (10 weeks old, SD rats, male) and treated them for 5 days under different magnitudes of orthodontic force to evaluate the change of PDL. In terms of experimental design, the white rats were classified according to the force magnitude to be applied: 0 (no force), 5, 10, and 30 gf, respectively. Each rat was treated individually to protect against any potential distortion of the designed appliances. Prior to fixing the appliances, tribromo-ethanol (2,3,4-tribromo-ethanol, 300 mg/kg) 3 cc was injected via IM for anesthesia after ether inhalation. Acid etching was treated on the tooth surface with 37% phosphoric acid, and irrigation was done with normal saline to prepare the tooth surface for resin bonding. Heads were rotated slightly to the lateral side and gauzes were prepared to separate the oral and nasal cavities during irrigation to ensure there was no airway obstruction.

Fig. 1 The photographs of the designed appliances; the springs for **a** 5 gf, **b** 10 gf, and **c** 30 gf force magnitudes, respectively. Each one is partially covered with a light curable hard resin. The *arrows* indicate the force direction. **d** The specially designed bracket with a center hole of 0.7 mm in diameter

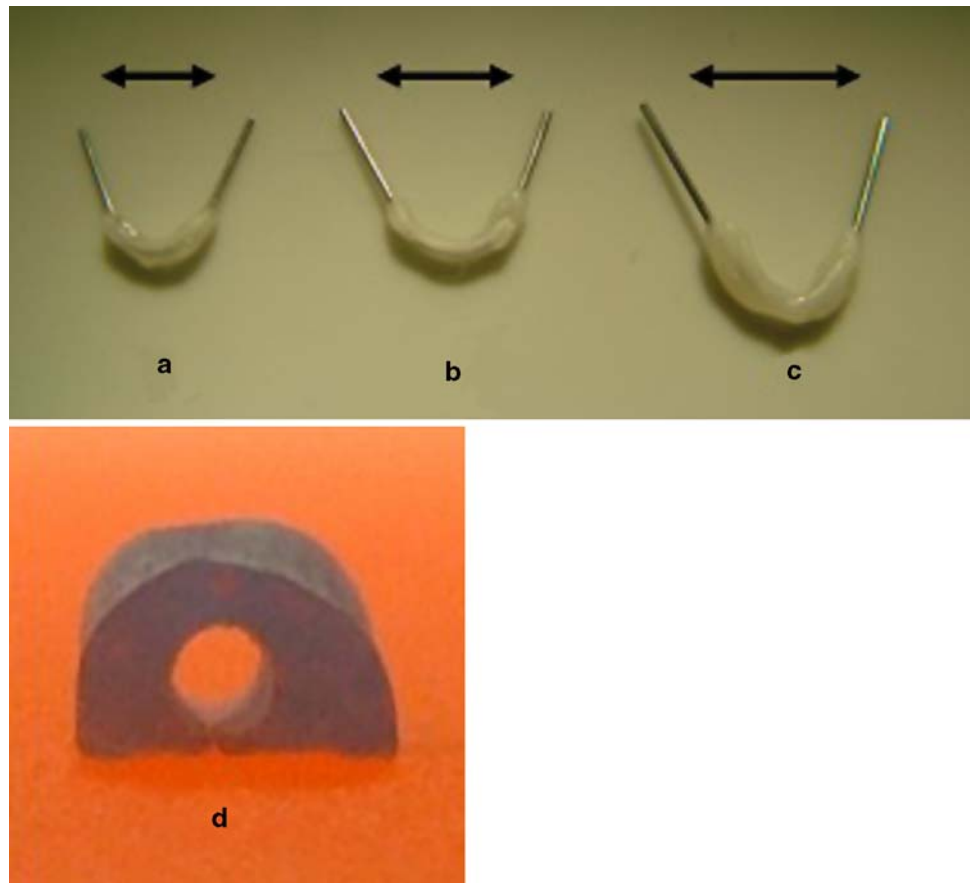


Table 1 Classification depending on the force magnitude and type of appliance

Group	Force magnitude (gf)	Type of appliance
Control	0	Plastic bracket ^a only
Light	5	0.014 Ni–Ti spring ^b
Medium	10	0.016 Ni–Ti spring
Heavy	30	0.018 Ni–Ti spring

^a Plastic bracket; specially designed resin bracket for rats

^b Ni–Ti spring; Jinsung Industrial Co. Ltd (Korea)

Figure 2 shows the designed spring installed into the bracket on the maxillary anterior teeth of the white rat. Here, the bonding positions on the lateral surface of the teeth were selected because the labial and lingual surfaces could be under the heavy irritation during mastication. The maxillaries were extracted for OCT and radiographic evaluations on the 5th day from the initial force application.

For the extraction of maxilla, the white rats were prepared for general anesthesia using the same method

Fig. 2 The designed memory-form-wire installed using the bracket and resin on the maxillary anterior teeth of a rat; front view (*left*), side view (*right*)



previously described, and the rats were subsequently euthanized. Circumferential incisions were then made in the upper vestibule area to separate the upper jaw from the skin. Next, a surgical microsaw connected to a low speed engine was used to separate the upper jaw from the skull at the area from the nasal cavity to the palatal bone, and the separated maxillaries were fixed in a formalin solution (neutral buffered 10%). It should be noted that all of these processes were done under the evaluation of and permission from the Institutional Animal Care and Use Committee, Ulsan University (Ulsan, Korea).

2.3 Experimental set-up

To evaluate the structural variation of PDL induced by the orthodontic forces, we performed noninvasive imaging in two ways; X-ray imaging was used as a conventional method, and OCT imaging was used as a high-resolution optical imaging approach. Since OCT can provide a cross-sectional high-resolution image without requiring the sectioning of samples, it was possible to carry out a sophisticated optical biopsy.

The schematic diagram of the OCT system employed in this experiment is shown in Fig. 3. The system utilizes a broadband light source with an output power of 4 mW, a center wavelength of $\lambda_c = 1310$ nm, and a bandwidth of $\Delta\lambda = 38$ nm. The optical power from the low coherent light source is split at the 3 dB fiber coupler and directed toward the sample and the reference arms of the fiber-based Michelson interferometer. The lights back-reflected from the reference mirror and back-scattered from the sample are then recombined at the same coupler and subsequently delivered to the detector.

An interferometric signal is detected only when the optical path length difference between both arms is less than the coherence length of the light source. A simple voice coil-driven positioning scanner and a precision

motorized stage are employed for varying the reference path length and for transverse scanning on the sample, respectively. A cross-sectional image is then obtained by transversely scanning the beam across the sample and detecting the power of the reflected light in terms of its depth along the sample at each transverse position. The interferometric signal from the detector is first processed with a bandpass filter to obtain a modulated signal with a minimum of noise. To extract the axial information of the sample, the signal is electronically demodulated thereby allowing only the envelope signal to be extracted. Then, the electrical signal is digitized by an acquisition board and constructed into a tomographic image with a personal computer.

To enhance the signal contrast, balancing the optical powers of the back-reflected signals from both arms is necessary. To adjust the reflected optical power from the reference arm, a neutral density filter or intentional misalignment in the reference arm is used. In this experiment, the axial and the lateral resolutions were measured to be 14 and 10 μm , respectively. The resolutions were sufficient for detecting the minute change of PDL spaces, an average thickness of 0.15–0.38 mm in the case of humans [1].

3 Results

The effect of orthodontic force on the ligament structure was evaluated by imaging the PDL region. Then, changes in the PDL were compared based on the images acquired using two imaging methods; intraoral digital X-ray radiography (Digital X-ray intra-oral sensor system, VATECH, Korea) and OCT. Figure 4 shows an optical photograph, a radiographic image, and an OCT image of the maxillary anterior tooth of the white rat in the control, to which no orthodontic force was applied. The arrow shown in Fig. 4a indicates the OCT scanning direction. As can be seen in Fig. 4b, c, the PDL of the white rat was too narrow to be clearly identified, and as such only the boundary between the epithelium and the tooth could be distinctly shown.

Variations in the PDL structures were, however, observed with OCT imaging when orthodontic forces were applied. Figure 5d–f shows the OCT images taken with different orthodontic forces. To fully appreciate the increased detail available in the images obtained with the OCT technique, the images taken with conventional radiography are shown in Fig. 5a–c; the arrows in the upper X-ray images indicate the direction of the sample scanning for subsequent OCT imaging. As can be seen in the figure, the X-ray images could show only the spaces between the teeth and the alveolar bone. However, the OCT images show the change of PDL structures much more clearly (Fig. 5b). It should be noted that the PDL structure was

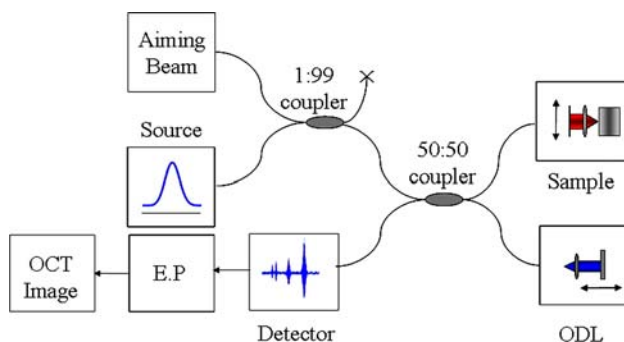


Fig. 3 Schematic diagram of the implemented fiber-based OCT system; *ODL* optical delay line, *EP* electrical processing

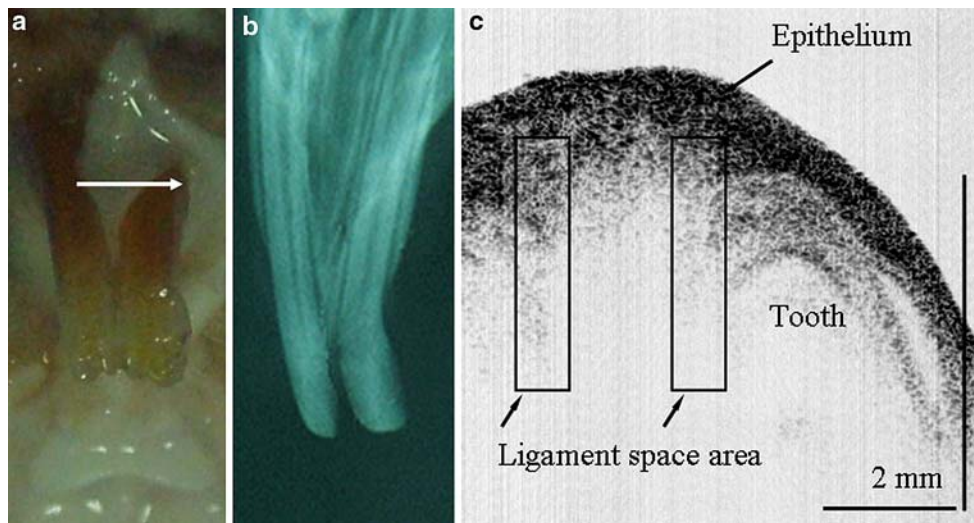
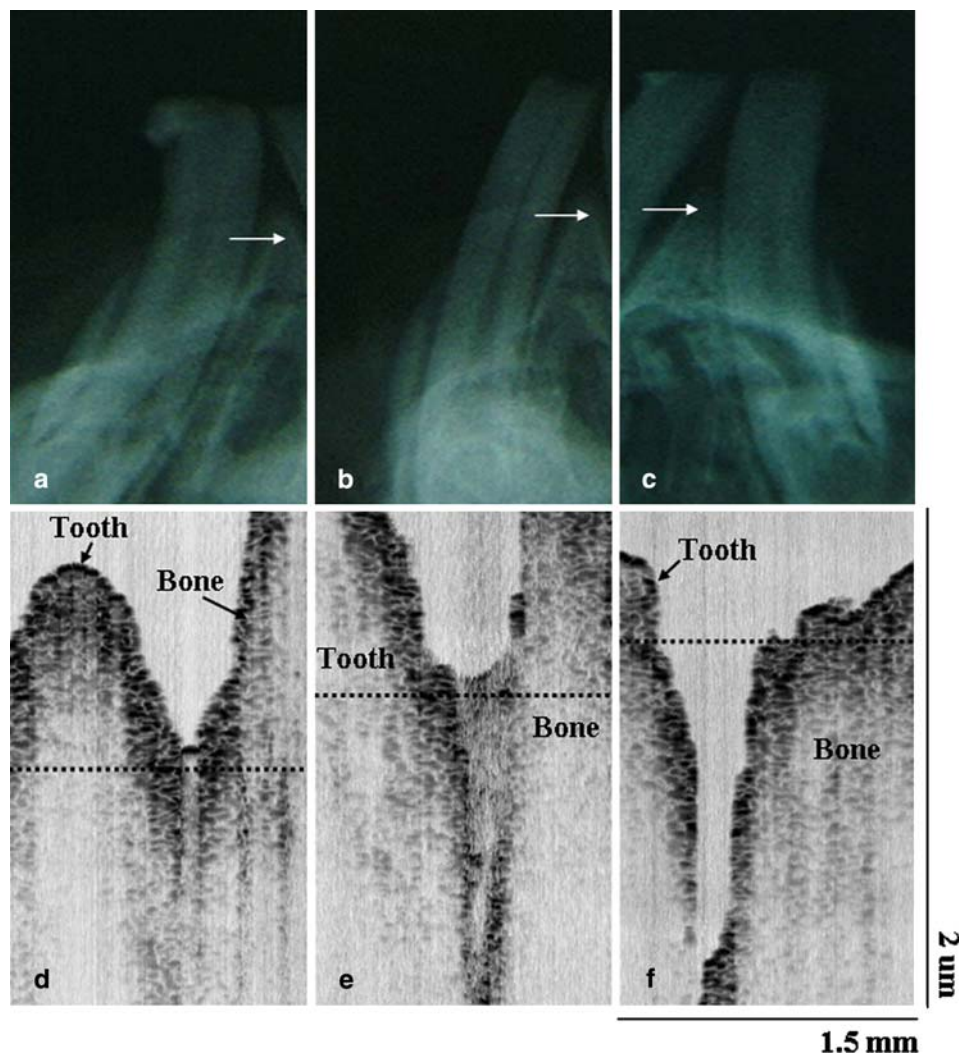


Fig. 4 Maxillary anterior tooth of a white rat in the control group, to which no orthodontic force was applied: **a** optical photograph; **b** radiographic image; **c** OCT image

Fig. 5 Radiographic (*top*) and OCT images (*bottom*) of the maxillary anterior teeth of white rats under several orthodontic forces: **a** and **d** 5 gf; **b** and **e** 10 gf; **c** and **f** 30 gf forces, respectively. The two-dimensional OCT image in the *bottom* was taken along the arrow direction in each of the *top* (radiographic) figures



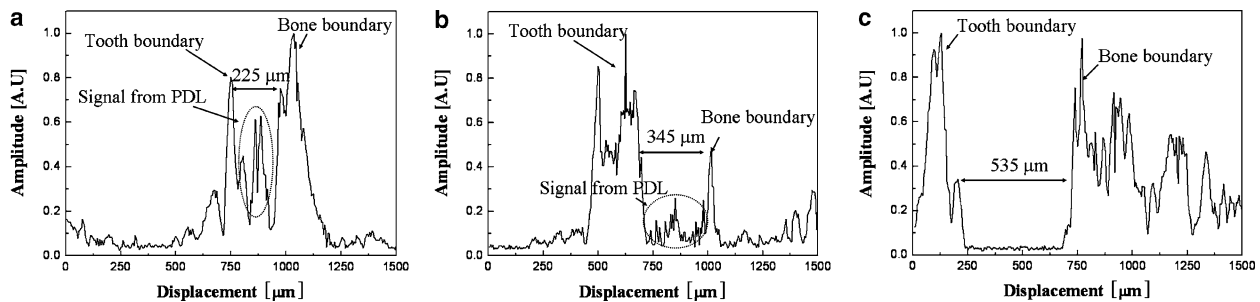


Fig. 6 The one-dimensional OCT images taken near the enlarged PDL structure; **a** light (5 gf), **b** medium (10 gf), and **c** heavy (30 gf) force magnitudes, respectively. The one-dimensional OCT image was taken along the *dotted line* in Fig. 5d–f

torn out when 30 gf force was applied, and that the measuring area of the image was 1.5 mm × 2 mm (transverse × axial).

Figure 6 shows the one-dimensional (thus, line) profiles of the PDL structure obtained from the acquired two-dimensional OCT raw data. The sectioned lines are indicated by the dotted lines in the images Fig. 5d–f, with a sectional profile length of 1.5 mm in each image. Each profile shows the change of the PDL structure with the applied force magnitude of 5, 10, and 30 gf, where it can be seen that the PDL was proportionally stretched with the orthodontic force, and variations of the space were measured to be 225, 345, and 535 μm, respectively. Our results indicate that in the case of the light force magnitude (5 gf), the amplitude of the signal back-reflected from PDL was relatively higher compared to the medium magnitude (10 gf), and that there was no signal from PDL for the heavy magnitude (30 gf).

4 Discussion and conclusions

Although continuous efforts have been made to apply OCT in the area of dentistry, the active or real-time monitoring of the PDL under various orthodontic forces, including functional or parafunctional forces, has been rarely reported to date. However, the use of OCT is potentially clinically valuable as a means of evaluating the active states of oral tissues during orthodontic treatment, especially with respect to the increased safety and convenience of patients. If a treatment procedure can be completed while continuously monitoring PDL response, a dentist will be able to more effectively choose optimum orthodontic forces, which can be different for different patients, thereby minimizing any discomfort faced by the patient and avoiding accidental PDL damage.

We aimed to evaluate the feasibility of using OCT in the field of active diagnosis for dentistry, as PDL is very sensitive to outer irritation and easily changed by the application of an external pressure. To verify this variance,

the teeth of a white rat were selected as the target samples in this study. The periodontal tissues of a white rat are quite active due to the fact that their tooth eruption cycle is only 8–10 days; the PDL space is basically the area between the rounded margins of a tooth root and its alveolar socket. In addition, the hard and the soft tissues of a rat are very thin, making them adequate for OCT examination. For these reasons, we selected the white (SD) rat as the best sample for an animal-based experiment.

In this experiment, we observed that the OCT signal amplitude of the PDL for the case involving a small orthodontic force was higher than for the case involving a larger force. This observation might be understood by considering the fact that PDL is composed of a sparse structure, mainly collagen. Therefore, relatively less light power could be back-scattered when the PDL was stretched more; in general, a sparse medium has less scattering than a dense one. The OCT image taken under the medium force magnitude (10 gf) showed a better image quality than under the light force (5 gf) magnitude. With the medium force, the PDL was suitably stretched and we could observe some vertical structures inside the PDL. In addition, through the use of OCT we also could observe the most-upper surface margin of the ligament.

In the OCT image of the control group, Fig. 4c, onto which no orthodontic force was applied, we observed only the boundary between the epithelium and the tooth. The PDL structure could not be observed. We believe that the imaging depth of the implemented OCT system was not sufficient for reaching the depth of the PDL, and as such we might have failed to image some sections of the samples, though unfortunate. Here, each group consisted of a different white rat. Thus, preparing the same representative sample from different rats was difficult, as was targeting the same sections for measurement. Based on these limitations, a more careful experiment might provide further detail of the PDL structure under no orthodontic force. It is thought that polarization-sensitivity OCT (PS-OCT) [6, 12, 16] could be helpful for subsequent PDL evaluation, because collagen is the main

component of PDL and well known as having a strong birefringence.

During the experiment, it was found that conventional X-ray radiography could not discriminate any variation of the PDL under orthodontic forces. It only showed the existence of the PDL space, from which detecting minute changes of the PDL was almost impossible.

To carry out a more sophisticated examination, we should evaluate the various effects of surface texture, the distance between different tissues, the composition of tissues, and the effect of moisture in the target sample. In addition, an OCT system having a better axial resolution and an improved signal-to-noise ratio could enable a more precise evaluation of a thinner PDL. It is noteworthy that the amount of PDL change around a rat tooth is smaller than the one in a human subject.

To be able to use OCT for clinical dentistry, of course, there are many tasks that remain to be overcome. However, from these experimental results, we believe that OCT can be used for *in vivo* evaluations of the PDL in human subjects, and has a great potential for use in the active diagnoses of many diseases that are related to changes of the PDL as a result of functional or parafunctional outer forces such as bruxism, temporomandibular joint disorder, root resorption, periodontal bone destruction, etc.

In this study, we have successfully observed variations of the PDL in the maxillary anterior teeth of white (SD) rats under different orthodontic force magnitudes by using a time-domain fiber-based OCT system. We believe that subsequent research will allow this potential to be realized in human subjects.

Acknowledgments This work was supported in part by the Ministry of Commerce, Industry and Energy of Korea through the Industrial Technology Infrastructure Building Program and by the Advanced Technology Center (ATC) project of the Ministry of Commerce Industry and Energy (MOCIE).

References

- Avery JK, Steele PF (2000) Essentials of oral histology and embryology: a clinical approach, 2nd edn. Mosby, St Louis, pp 133–143
- Böhl MV, Maltha J, den Hoff HV, Kuijpers-Jagtman AM (2004) Changes in the periodontal ligament after experimental tooth movement using high and low continuous forces in beagle dogs. *Angle Orthod* 74:16–25
- Ciancio SC, Neiders ME, Hazen SP (1967) The principal fibers of the periodontal ligament. *Periodontics* 5:76–81
- Colston BW Jr, Sathyam US, Silva LBD et al (1998) Dental OCT. *Opt Express* 6:230–238
- Choma MA, Sarunic MV, Yang C, Izatt JA (2003) Sensitivity advantage of swept source and Fourier domain optical coherence tomography. *Opt Express* 11:2183–2189
- de Boer JF, Milner TE, Van Gemert MJC, Nelson JS (1997) Two-dimensional birefringence imaging in biological tissue by polarization-sensitive optical coherence tomography. *Opt Lett* 22:934–936
- de Boer JF, Cense B, Park BH et al (2003) Improved signal to noise ratio in spectral domain compared with time domain optical coherence tomography. *Opt Lett* 28:2067–2069
- Feldchtein FI, Gelikonov GV, Gelikonov VM et al (1998) *In vivo* OCT imaging of hard and soft tissue of the oral cavity. *Opt Express* 3:239–250
- Feldchtein FI, Gelikonov GV, Gelikonov VM et al (1998) Endoscopic applications of optical coherence tomography. *Opt Express* 3:257–270
- Fujimoto JG (2003) Optical coherence tomography for ultrahigh resolution *in vivo* imaging. *Nat Biotechnol* 21:1361–1367
- Huang D, Swanson EA, Lin CP et al (1991) Optical coherence tomography. *Science* 254:1178–1181
- Hee MR, Huang D, Swanson EA, Fujimoto JG (1992) Polarization-sensitive low-coherence reflectometer for birefringence characterization and ranging. *J Opt Soc Am B* 9:903–908
- Khouw FE, Goldhaber P (1970) Changes in vasculature of the periodontium associated with tooth movement in the rhesus monkey and dog. *Arch Oral Biol* 15:1125–1132
- Otis LL, Everett MJ, Sathyam US, Colston BW Jr (2000) Optical coherence tomography—a new imaging technology for dentistry. *J Am Dent Assoc* 131:511–514
- Podoleanu AG, Rogers JA, Jackson DA, Dunne S (2000) Three dimensional OCT images from retina and skin. *Opt Express* 7:292–298
- Pasquesi JJ, Schlachter SC, Boppart MD et al (2005) *In vivo* detection of exercise-induced ultrastructural changes in genetically-altered murine skeletal muscle using polarization-sensitive optical coherence tomography. *Opt Express* 14:1547–1556
- Rygh P, Reitan K (1972) Ultrastructural changes in the periodontal ligament incident to orthodontic tooth movement. *Trans Eur Orthod Soc* 1972:393–405
- Ren Y, Maltha JC, Kuijpers-Jagtman AM (2003) Optimum force magnitude for orthodontic tooth movement: a systematic literature review. *Angle Orthod* 73:86–92
- Ren Y, Maltha JC, Kuijpers-Jagtman AM (2004) The rat as a model for orthodontic tooth movement—a critical review and a proposed solution. *Eur J Orthod* 26:483–490
- Schuman JS, Puliafito CA, Fujimoto JG (2004) Optical coherence tomography of ocular diseases. Slack, Thorofare
- Tearney GJ, Brezinski ME, Southern JF et al (1997) Optical biopsy in human urologic tissue using optical coherence tomography. *J Urol* 157:1915–1919
- Tumlinson AR, Barton JK, Považay B et al (2006) Endoscope-tip interferometer for ultrahigh resolution frequency domain optical coherence tomography in mouse colon. *Opt Express* 14:1878–1887
- Wennstrom JL, Lindhe J, Sinclair F, Thilander B (1987) Some periodontal tissue reactions to orthodontic tooth movement in monkeys. *J Clin Periodontol* 14:121–129
- Wang XJ, Milner TE, de Boer JF et al (1999) Characterization of dentin and enamel by use of optical coherence tomography. *Appl Optics* 38:2092–2096
- Wojtkowski M, Srinivasan V, Fujimoto JG et al (2005) Three-dimensional retinal imaging with high-speed ultrahigh-resolution optical coherence tomography. *Ophthalmology* 112:1734–1746
- Zeichner SJ, Ruttimann UE, Webber RL (1987) Dental radiography: efficacy in the assessment of intraosseous lesions of the face and jaws in asymptomatic patients. *Radiology* 162:691–695